



## Synthesis of New Quinoxaline Pharmacophores as Antitumor Agents on MCF-7 breast cancer cells

Elsherbiny S. El-sayed<sup>1</sup>, Ahmed S. Saad<sup>2</sup>, Sara A. Abu El-ata<sup>1,\*</sup>

<sup>1</sup> Chemistry department, Faculty of Science, Port Said University, Port Said 42526, Egypt

<sup>2</sup> Pharmacology and Toxicology department, Faculty of Pharmacy, Port Said University, Port Said 42526, Egypt

\*Corresponding author: [sara\\_adel174@yahoo.com](mailto:sara_adel174@yahoo.com)

### ABSTRACT

A new first series from 2-substituted quinoxalines (3-6) were synthesized using o-phenylenediamine with aryl bromomethyl ketones as a key starting material. Moreover, a new second series from 2-oxo-1,2,3,4-tetrahydro-benzo [g] quinoxaline (8-10) were obtained from the reaction of naphthalene-2,3-diamine with ethyl chloroacetate. The structures of the two compound types were confirmed by spectral data studies along with elemental microanalysis. The cytotoxic effects of the synthesized compounds were tested using a MTT colorimetric assay against MCF-7 cells. Four of the compounds, given numbers 4, 5, 9 and 10, were found to induce significant levels of cytotoxicity. Compounds number 5 and 9 showed promising assay results and were tested in the non-cancerous cell line MCF-10A and neither of them showed cellular deterioration. Furthermore, compound 9 was reported to suppress tubulin polymerization. These findings were confirmed by the docking study results demonstrating a remarkable binding affinity of compound 9 to tubulin active site. These findings suggest that compound 9 has a pharmacological potential as an antineoplastic drug in MCF-7 cells.

### Keywords:

Microtubules, Quinoxaline, Breast Cancer, Tubulin.

### 1. INTRODUCTION

Globally, breast cancer is the most often diagnosed cancer. Carcinoma is that the second leading reason behind cancer related deaths in females and therefore the fifth leading reason for cancer mortality in both sexes [1]. Triple negative breast cancer (TNBC), Human Epidermal growth factor Receptor 2-enriched breast cancer, and hormone receptor-positive breast cancer are among the molecular subtypes of breast cancer that have been classified [2][3]. Recently, extensive efforts have been globally made towards the discovery of more effective novel therapeutic modalities for breast cancer that hopefully could increase the survival rate.

Primarily, microtubules are integral components of eukaryotic cell cytoskeleton that are remarkably crucial in cellular activities such as migration and proliferation [4].

Notably, the activity of microtubules is intimately linked to the functional properties of malignant cells, including aberrant mitotic division rate, invasion of neighboring tissue, and metastasis. Tau proteins and other tubulin-associated proteins regulate the polymerization of  $\alpha$  and  $\beta$ -tubulin dimers, which make up microtubules [5]. Many anticancer medications, including vincristine, vinblastine, and paclitaxel, work by targeting the cytoskeleton of microtubules [6]. Consequently, microtubules are a desirable pharmacological target for the creation of novel antimitotic drugs in the study of anticancer therapy.

In the dye, pharmaceutical, agrochemical, and material sectors, heterocyclic chemicals like quinoxaline and quinazoline derivatives are important building blocks [7][8][9][10]. Numerous medications, such as antiviral, anticancer, and antiemetic medications, have been shown to include nitrogen heterocycles [11]–[16]. A few techniques, including oxidation-trapping of  $\alpha$ -hydroxy ketones with 1,2-diamines, cyclization-oxidation of phenacyl bromides, and oxidative coupling of epoxides with phenylene-1,2-diamines, have been reported for the production of substituted quinoxalines [17]–[19]. Numerous heterogeneous and homogeneous catalysts were described for the synthesis of quinoxaline derivatives from the condensation of primary alcohols or vicinal diols with diamines [22]–[27] following the introduction of the hydrogen borrowing approach [20], [21].

Given that cancer is the primary cause of death and morbidity in the globe, the US Patent Office and WIPO (PCT) have received numerous applications for and grants of patents pertaining to quinoxaline nucleus. The majority of the patents discussed the synthesis and use of novel quinoxaline derivatives in the management of different cancer kinds [28]. A few notable patent examples are displayed in (Fig. 1).

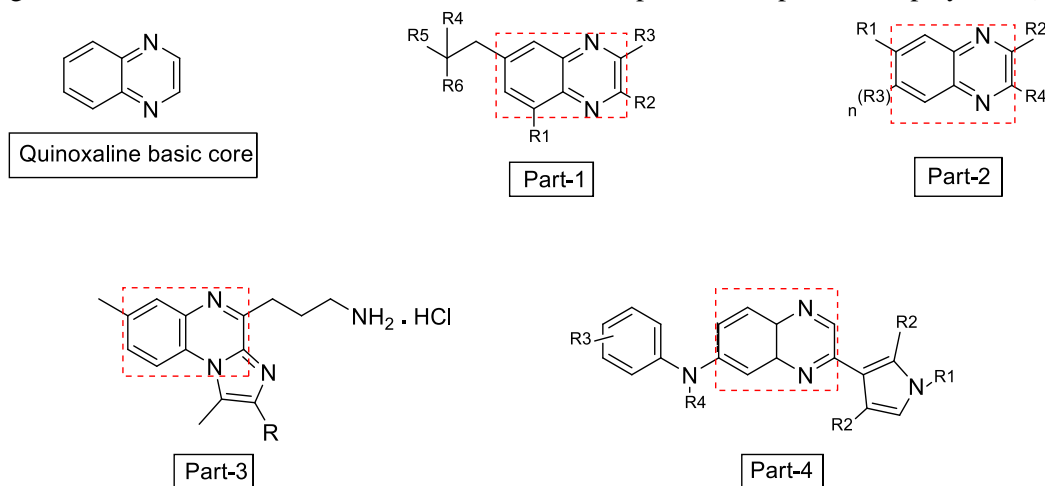


**Fig. 1:** Structure of Examples of quinoxaline-based patented molecules

As mentioned earlier, tubulin polymer-based microtubules, which are in a state of dynamic equilibrium with tubulin dimers, are essential for mitotic cell division. Therefore, apoptosis and cell cycle arrest can result from cancer cells' targeting microtubule production. One of the best targets for the creation of innovative anti-cancer chemotherapeutic drugs is said to be microtubules. Fig. 2 shows some of the 1,2,3,4 tetrahydraquinoxalin-2-one compounds as examples for antitubulin agents [29].

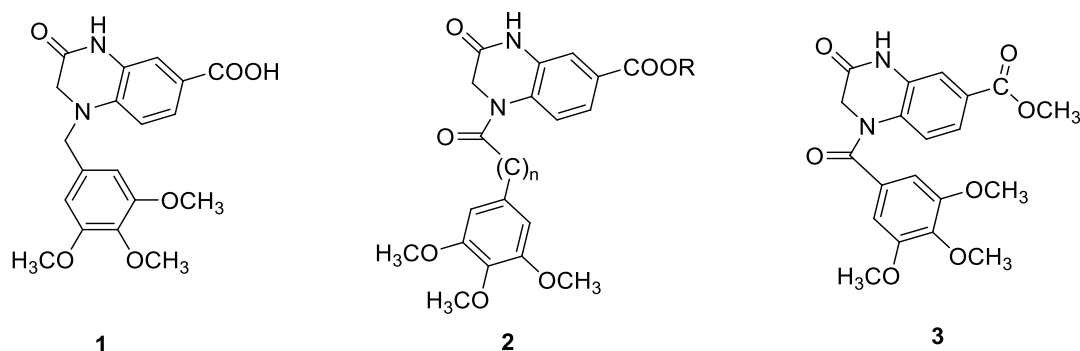


**Fig. 2:** Tetrahydroquinoxalin-2-ones motifs targeting tubulin dynamics.

In this research, we have synthesized two novel quinoxaline derivatives as shown in (Fig. 3). and examined their characteristics as novel antitumor agents [30-31]. The two synthesized quinoxaline derivatives were assessed in in-vitro assays in MCF-7 breast cancer cells.



**Fig. 3:** A) 2-Substituted quinoxaline molecules (type 1).

B) Tetrahydrobenzo[g] quinoxaline-2-one molecules (type 2).

## 2. MATERIALS AND METHODS

**2.1 Chemistry:** Unless specified otherwise, all compounds were obtained from commercial sources and utilized without additional purification. Using the KBr disc approach, the infrared data were collected in a Jasco FIT IR 6100 infrared spectrometer. The Bruker 400 DRX-Avance NMR spectrometer was used to measure the <sup>1</sup>H- and <sup>13</sup>C-NMR (400 MHz) spectra. All chemical shifts were reported in ppm with respect to tetramethylsilane. Using an electrothermal melting point equipment, the melting point of the produced compounds was determined and has not been adjusted. Utilizing a Finnigan MATSSQ-700 mass spectrometer, mass spectra were ascertained. Using a variety of elemental techniques, elemental microanalyses were conducted at the Central Services Laboratory, National Research Center, Dokki, Cairo, Egypt, and the results were found to be within  $\pm 0.5\%$  of the theoretical values.

**2.1.1 Preparation of aryl bromomethyl ketones (2a, b):** 4-bromo-2-hydroxyphenyl bromide (2a) and 3,5-dibromo-4-aminophenacyl bromide (2b) were prepared *via* the halogenation of 2-hydroxyacetophenone and 4-aminoacetophenone with bromine in glacial acetic acid according to literature methods [32].

**2.1.2 General procedure for the synthesis of compounds 3 and 4:** A mixture of compound 2a and / or 2b (0.01 mole), *o*-phenylene diamine (0.01 mole) and fused sodium acetate (0.03 mole) in acetic acid (25 ml) was heated under reflux for 4h, monitored by Thin Layer Chromatography (TLC). The reaction mixture was cooled, poured into water with stirring, and the solid formed was isolated by filtration. The crude product was recrystallized from ethanol to give 3 and 4.

2-(4-bromo-2-hydroxy) phenyl quinoxaline (3) as yellow crystals, yield 71%, m.p.180 °C. IR (KBr)  $\gamma_{\max}$  =3456 (br.OH), 1633 (C=N), 1605,1583 (C=C), 1121, 1063 (C-O)  $\text{cm}^{-1}$ .  $^1\text{H}$ NMR (DMSO-*d*6)  $\delta$ : 7.03-8.25 (m, 7H, Ar-H of 2 stereo isomers), 9.72 (s,1H, CH=N), 12.17 (br. S, 1H, OH, Z-isomer), 12.49 (s, 1H, OH, E-isomer).  $^{13}\text{C}$  NMR (DMSO-*d*6)  $\delta$ :159.05, 157.62 (C-O of two isomers),152.26, 150.85 (C=N of two isomers), 145.82, 145.45 (C=N of two isomers), 141.05, 140.81, 140.19, 139.63, 138.60, 135.06, 131.40, 130.73, 130.41, 129.62, 129.33, 128.95, 128.59, 123.02, 120.50, 120.09, 120.04, 119.97, 118.03, 111.26, CC aromatic of two isomers I2 and Z) ppm.

MS: m/z (%) =302 ( $\text{M}^+ +2$ , 14.09), 301 ( $\text{M}^+ +1$ , 11.94), 300 ( $\text{M}^+$ , 15.64), 274 (0.98), 273 (0.68), 272 (1.60), 223 (20.30), 222 (100), 221 (92.97), 194 (28.71), 193 (35.30), 192 (11.31), 191 (3.45), 140 (3.05), 139 (4.72), 129 (1.64), 111 (2.24), 110 (3.44), 103 (3.30), 102 (3.88), 97 (2.61), 96 (2.79), 91(2.73), 83(1.14), 77 (5.12), 76 (4.90), 75 (2.18), 63 (1.44). Anal. calcd. for  $\text{C}_{14}\text{H}_9\text{N}_2\text{BrO}$  (300): C, 56.00; H3.00; N, 9.33. Found: C 35.88; H, 2.78; N, 9.01.

2-(3,5-Dibromo-4-amino) phenyl quinoxaline (4) as yellow crystals, yield 76%, m.p.205 °C. IR (KBr)  $\gamma_{\max}$  = 3365, 3189 ( $\text{NH}_2$ ), 1636 (C=N), 1611, 1583 (C=C)  $\text{cm}^{-1}$ .  $^1\text{H}$ NMR (DMSO-*d*6) $\delta$ : 5.88(s, 2H,  $\text{NH}_2$ ), 7.75-8.04 (m, 4H, Ar-H), 8.39 (s, 2H, Ar-H), 9.44 (s, 1H, CH=N) ppm.  $^{13}\text{C}$  NMR (DMSO-*d*6): 148.48, 145.23 (2\* $\text{C}=\text{N}$ ), 143.45, 141.70, 141.09 (3\*  $\text{C}=\text{N}$ ) 131.16, 131.08, 129.29, 129.14, 126.39, 108.35 (C-aromatic) ppm. MS: m/z (%) =381 ( $\text{M}^+ +4$ , 71.27), 380 ( $\text{M}^+ +3$ , 50.12), 379 ( $\text{M}^+ +2$ , 97.58), 378 ( $\text{M}^+ +1$ , 100), 377 ( $\text{M}^+$ , 46.03), 376 ( $\text{M}^+ -1$ , 52.62), 352 (5.61), 351 (8.41), 350 (3.45), 349 (5.84), 335 (2.77), 302 (1.67), 301 (13.18), 300 (27.35), 299 ( 17.69), 298 (16.50), 297 (13.99), 278 (14.80), 277 (9.48), 276 (27.62), 274 (16.37), 273 (19.42), 271 (14.35), 246 (2.55), 244 (2.57), 220 (3.28), 219 (13.44), 218 (15.44), 217 (6.99), 193 (8.77), 192 (34.64), 191 (9.67), 190 (7.75), 189 (9.47), 188 (4.99), 165 (9.57), 164 (6.82), 150 ( 2.96), 149 (2.87), 116 (3.53), 115 (5.69), 114 ( 1.58), 76 (2.41). Anal. calcd. for  $\text{C}_{14}\text{H}_9\text{N}_3\text{Br}_2$  (377): C, 44.52; H 2.39; N, 11.14. Found: C, 44.33; H, 2.11; N, 11.01.

### 2.1.3 General procedure for the acylation reaction

**Synthesis of compounds 5 and 6:** A solution of compound 3 and /or 4 (0.01 mole) in acetic anhydride (15 ml) was heated at 100 °C for 2 hr. then reaction mixture was cooled, poured into ice-water with stirring and left for 24 hr. The resulting solid residue was filtered off, washed with water, dried and purified by recrystallization from benzene to give compounds 5 and 6.

2-(4-Bromo-2-acetoxy) phenyl quinoxaline (5) as colorless crystals, yield 68 %, m.p 152 ° C. IR (KBr)  $\gamma_{\max}$  = 1763 (C=O), 1632 (C=N), 1608, 1587 (C=C), 1113, 1066 (C-O)  $\text{cm}^{-1}$ .  $^1\text{H}$ NMR(DMSO-*d*6) $\delta$ : 2.22 (s, 3H,  $\text{COCH}_3$ ), 7.37-7.39 (d, 1H, Ar-H), 7.83-7.96 (m, 3H, Ar-H), 8.15-8.19 (m, 3H, Ar-H), 9.26 (s, 1H, CH=N) ppm (**Fig. 4**).  $^{13}\text{C}$  NMR (DMSO-*d*6): 169.48 (C=O), 149.51 (C-O) 148.16, 145.74 141.72, 141.28 (2\*  $\text{C}=\text{N}$  and 2\* $\text{C}-\text{N}$ ) 134.12, 133.84, 132.30, 131.42, 131.26, 129.74,129.39, 126.71, 119.31 (C-aromatic), 21.19 ( $\text{CH}_3$ ) ppm. MS: m/z (%) = 344 ( $\text{M}^+ +2$ , 2.07), 343 ( $\text{M}^+ +1$ , 1.14), 342 ( $\text{M}^+$ , 2.50), 316 (2.08), 315 (3.50), 314 (3.40), 313 (2.52), 312 (1.44), 303 (10.09), 302 (83.21), 301 (51.39), 300 (100), 299 (44.29), 274 (3.66), 273 (2.88), 272 (5.28), 271 (2.21), 247 (1.23), 245 (1.30), 222 (3.47), 221 (4.69), 220 (8.54), 219 (2.59), 205 (1.91), 194 (4.47), 193 (20.32), 192 (12.79), 191 (4.52), 166 (3.64), 165 (2.76), 164 (6.69), 140 (1.12), 139 (1.77), 138 ( 1.51), 131 (1.14), 129, (1.34), 103 (2.11), 102 (6.77), 77 (2.98), 76, (3.71), 75 (1.91), 63 (1.27). Anal. calcd. for  $\text{C}_{16}\text{H}_{11}\text{N}_2\text{BrO}_2$  (342): C, 56.14; H 3.21; N, 8.19. Found: C, 55.89; H, 3.01; N, 8.08.

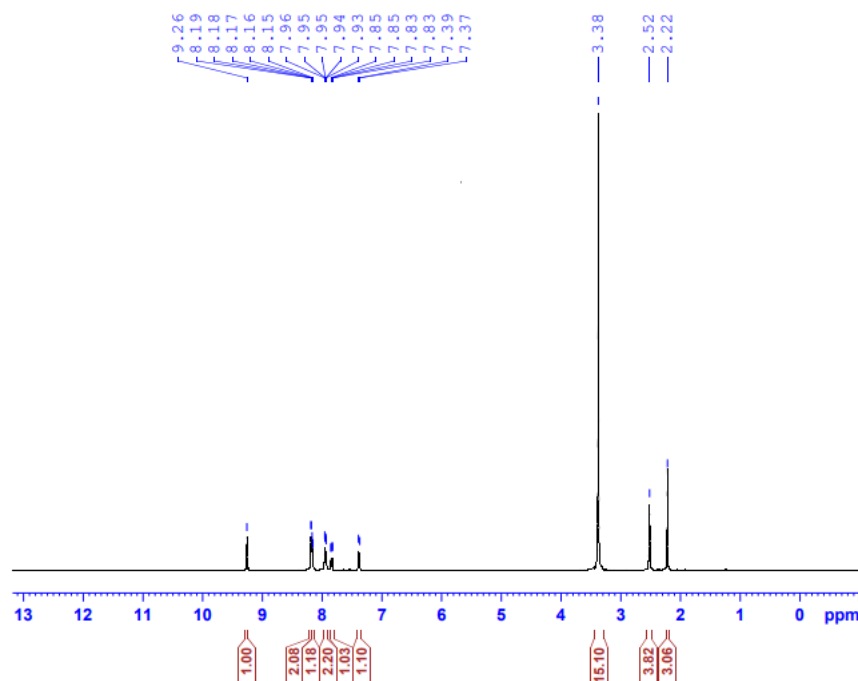


**Fig. 4:**  $^1\text{H}$ NMR of 2-(4-Bromo-2-acetoxy) phenyl quinoxaline

2-(3,5-Dibromo-4-acetylamino) phenyl quinoxaline (**6**) as pale-yellow crystals, yield 61 %, m.p 233 °C. IR (KBr)  $\gamma_{\text{max}}$  = 3225 (NH), 1648 (C=O), 1633 (C=N), 1608, 1582 (C=C)  $\text{cm}^{-1}$ .  $^1\text{H}$ NMR (DMSO-*d*<sub>6</sub>) $\delta$ : 2.11 (s, 3H, COCH<sub>3</sub>), 2.17 (s, 3H, COCH<sub>3</sub>), 5.96 (s, 1H, OH), 7.77-8.11 (m, 4H, Ar-H), 8.47-8.66 (s, 2H, Ar-H), 9.55-9.66 (s, 1H, CH=N of two isomers) ppm.  $^{13}\text{C}$  NMR (DMSO-*d*<sub>6</sub>): 168.55, 149.01, 145.32, 144.26, 143.61, 141.91, 141.75, 141.63, 141.19, 131.87, 131.39, 131.23, 131.12, 131.02, 129.83, 129.36, 129.23, 126.38, 125.46, 108.37 (6C) -aromatic, 23.06 (CH<sub>3</sub>) ppm.

Anal. calcd. for C<sub>16</sub>H<sub>11</sub>N<sub>3</sub>Br<sub>2</sub>O (41): C, 45.82; H, 2.63; N, 10.02. Found: C, 45.64; H, 2.41; N, 9.89.

**Preparation of 1,2,3,4- tetrahydro-2-oxo-benzo[9]quinoxaline (8):** Preparation: After being heated under reflux for four hr., a combination of 2,3 naphthalene diamine (0.01 mole), ethyl chloroacetate (0.01 mole), and fused sodium acetate (0.03 mole) in ethanol (30 mL) was chilled and then added to water while stirring. The solid product formed was filtered off, washed with water dried and purified by recrystallization from ethanol to give compound **8** as pale-yellow crystals, yield 71%, m.p 187 °C. IR (KBr)  $\gamma_{\text{max}}$  = 3252 (NH), 3380-2980 (br.OH), 1608, 1591 (C=C), 1063 (C-O)  $\text{cm}^{-1}$ .  $^1\text{H}$ NMR (DMSO-*d*<sub>6</sub>) $\delta$ : 3.77 (s, 2H, NH<sub>2</sub>CO), 4.93 (br. s, 2H, 2\*NH), 6.29 (s, 1H, CH of quinoxaline ring), 6.74-7.50 (m, 7H, Ar-H and OH), 10.59 (s, 1H, NHCO) ppm.  $^{13}\text{C}$  NMR (DMSO-*d*<sub>6</sub>): 167.05 (C=O), 137.91 135.59, 131.29 (3C-N), 128.89, 127.81, 126.89, 125.65, 124.97, 124.80, 122.82, 121.73, 110.92, 107.63. 107.26 (C- of aromatic for four isomers), 45.59 (NCH<sub>2</sub>CO) ppm. MS: m/z (%) = 199 (M<sup>+</sup> +1, 3.59), 198 (M<sup>+</sup>, 54.66), 342 (M<sup>+</sup>-1, 5.12), 170 (1.12), 169 (76.57), 168 (7.52), 159 (1.61), 158 (100), 157 (3.36), 141 (6.53), 140 (8.33), 139 (1.75), 131 (1.72), 130 (42.08), 129 (5.22), 115 (9.08), 114 (2.75), 113 (2.00), 103 (1.00), 102 (1.77), 97.(1.15), 84 (1.82), 70 (1.04), 69 (1.17). Anal. calcd. for C<sub>12</sub>H<sub>10</sub>N<sub>2</sub>O (198): C, 72.73; H 5.05; N, 14.14. Found: C, 72.57; H, 4.86; N, 14.02

**The procedure for the preparation of compound 9:** A mixture of compound **8** (0.01 mole), ethyl 3-(4-hydroxy-3-methoxy phenyl)-2-cyanoacrylate (0.01mole) on sodium acetate (0.03 mole) in ethanol (50 mL) was heated under reflux for 6 hr. The reaction mixture was cooled and poured into water with stirring, the formed crude residue was separated by filtration and purified with ethanol to give compound

9 as yellow crystals, yield 72%, m.p 126 °C. IR (KBr)  $\gamma_{\max}$  = 3405-2981 (br.OH), 3222 (NH), 2225 (CN), 1742, 1689 (C=O), 1615, 1586 (C=C), 1167, 1083, 1062 (C-O)  $\text{cm}^{-1}$ .  $^1\text{H}$ NMR (DMSO-*d*<sub>6</sub>)  $\delta$ : 1.30 (t, 3H, CH<sub>3</sub>), 4.30 (q, 2H, OCH<sub>2</sub>), 6.95-8.43 (m, 9H, Ar-H), 10.56 (s, 1H, NH) ppm (**Fig. 5**).  $^{13}\text{C}$  NMR (DMSO-*d*<sub>6</sub>): 163.64, 163.11 (C=O), 155.56, 155.43, 155.23, 153.23, 153.20, 153.18 (C-O), 148.6, 148.27, 133.99, 132.19, 130.43, 130.40, 129.74, 129.15, 128.61, 128.38, 128.31, 127.75, 127.61, 127.19, 125.30, 124.94, 123.31, 117.11, 116.49, 111.83, 111.49 (carbons of aromatic), 97.48 (C=N), 62.43 (OCH<sub>3</sub>), 14.54 (CH<sub>3</sub>) ppm. MS: m/z (%) = 443 (M<sup>+</sup>, unstable), 248 (4.86), 247 (5.95), 234 (3.45), 233 (20.60), 232 (2.32), 220 (1.99), 219 (26.95), 218 (2.41), 202 (16.96), 201 (1.07), 196 (7.83), 190 (3.11), 177 (3.98), 176 (18.41), 175 (9.10), 171 (5.57), 170 (33.81), 168 (3.88), 160 (2.59), 159 (5.75), 158 (15.95), 148 (2.18), 134 (1.23), 133 (3.36), 132 (10.51), 131 (2.31), 130 (5.72), 114 (15.71), 105 (3.02), 104 (4.99), 103 (6.76), 102 (3.41), 92 (2.36), 91 (1.98), 90 (2.03), 89 (3.02), 77 (4.37), 76 (11.47), 63 (2.83), 62 (1.74), 53 (2.21), 52 (4.45), 51 (2.16), 50 (3.56). Anal. calcd. for C<sub>25</sub>H<sub>2</sub>N<sub>3</sub>O<sub>5</sub> (443): C, 67.72; H 4.74; N, 9.48. Found: C, 67.46; H, 4.55; N, 9.29.

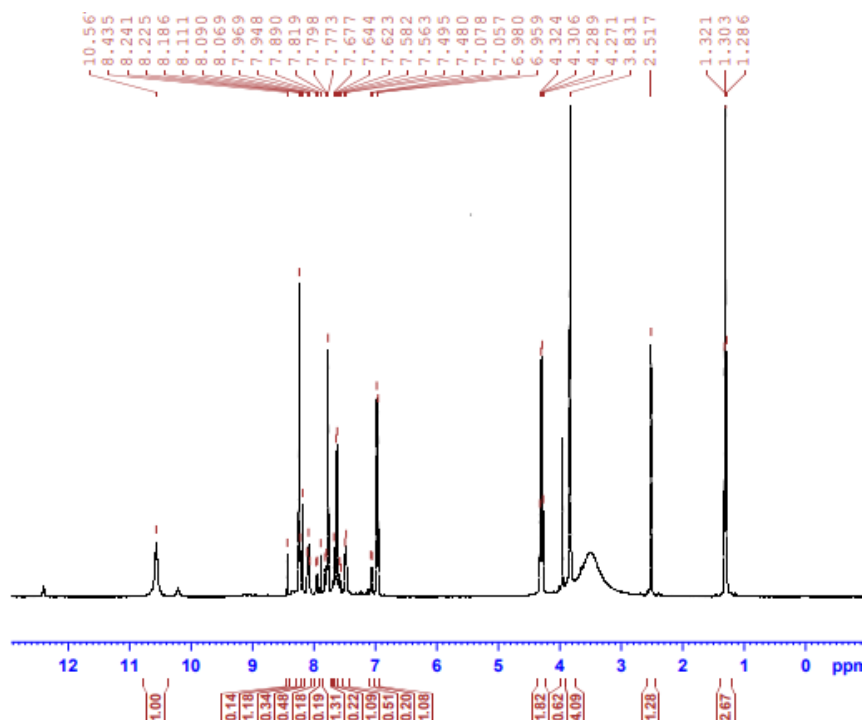


**Fig. 5:**  $^1\text{H}$ NMR of Compound (Z)-ethyl 2-cyano-3-(4-hydroxy-3-methoxyphenyl)-3-(3-oxo-3,4-dihydrobenzo[g]quinoxalin-1(2H)-yl) acrylate (9)

**Synthesis of compound 10:** A mixture of “compound 8 (0.01 mol), 4-chloro phenacyl bromide (0.01 mol)” in ethanol (30 mL) in the presence of triethylamine (1 mL) was heated under reflux for 6 hr. The reaction was cooled, poured into water and neutralized with diluted hydrochloric acid (2%). The resulting solid was filtered off, washed with water, dried and recrystallized from ethanol to give 10 as pale-yellow crystals, yield 63%, m.p 226 °C. IR (KBr)  $\gamma_{\max}$  = 3211(NH), 16113, 1586 (C=C), 1050 (C-O)  $\text{cm}^{-1}$ .  $^1\text{H}$ NMR (DMSO-*d*<sub>6</sub>) $\delta$ : 7.66-7.71 (m, 5H, Ar-H and H- quinoxaline), 8.81 (s, 2H, Ar-H), 9.65 (s, 1H, NH) ppm (**Fig. 6**).  $^{13}\text{C}$  NMR (DMSO-*d*<sub>6</sub>): 150.51 (C-O), 145.33, 138.32, 138.12, 136.19, 135.37, 134.21, 133.77, 129.86, 129.71, 128.90, 128.80, 127.72, 127.67, 127.54 (carbons of aromatic and oxazolopiperazine). MS: m/z (%) = 332 (M<sup>+</sup>, unstable), 293 (3.85), 292 (16.27), 291 (10.67), 290 (58.64), 289 (3.63), 275 (2.24), 274 (15.51), 255 (4.58), 231 (2.56), 228, (6.05), 227 (1.49), 201 (1.59), 200 (1.08), 196 (1.25), 152 (1.54), 145 (1.14), 141 (1.73), 140 (6.57) (12.91), 138 (2.59), 137 (26.89), 127 (14.76),



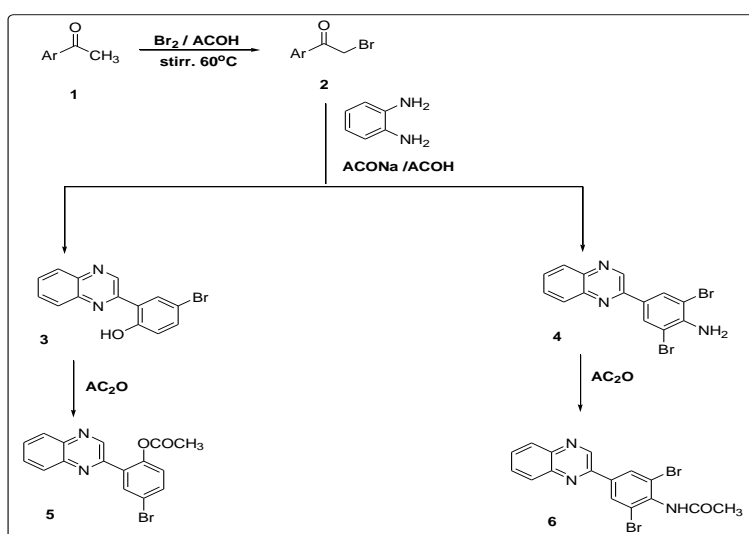
**2.3. Determination of tubulin beta using enzyme linked immunosorbent assay:** Tubulin beta inhibitory activity was quantitatively assessed *in-vitro* using ab245722 Human Beta-Tubulin SimpleStep ELISA® Kit (Abcam, Cambridge, UK), following the manufacturer's directions [34]. The results were expressed as IC<sub>50</sub> values (The required concentration to realize 50% inhibition of enzyme activity) using dose response curves and linear regression equation. The values presented were the means ( $\pm$  SD) of triplicate experiments.

**2.4 Molecular docking studies:** The tubulin structure (PDB code: 1SA0) [35] was retrieved from protein data bank. The docking study was carried out on Compound 9 beside colchicine. The docking procedures were performed using AutoDock Vina [36]. Marvin Sketch V19.12 was used for drawing ligand structures and the most energetically favored conformer was used for the next steps. The procedure for docking simulation was according to our previous study steps [37]. The grid boxes of center (x=118.9, y=89.7 and z= 5.9) with size (x=18.5, y=20.2, z=16.1) were used to define the active site. AutoDock Vina was executed. using Discovery Studio client was used for visualization and interpretation of the ligand-tubulin interactions.

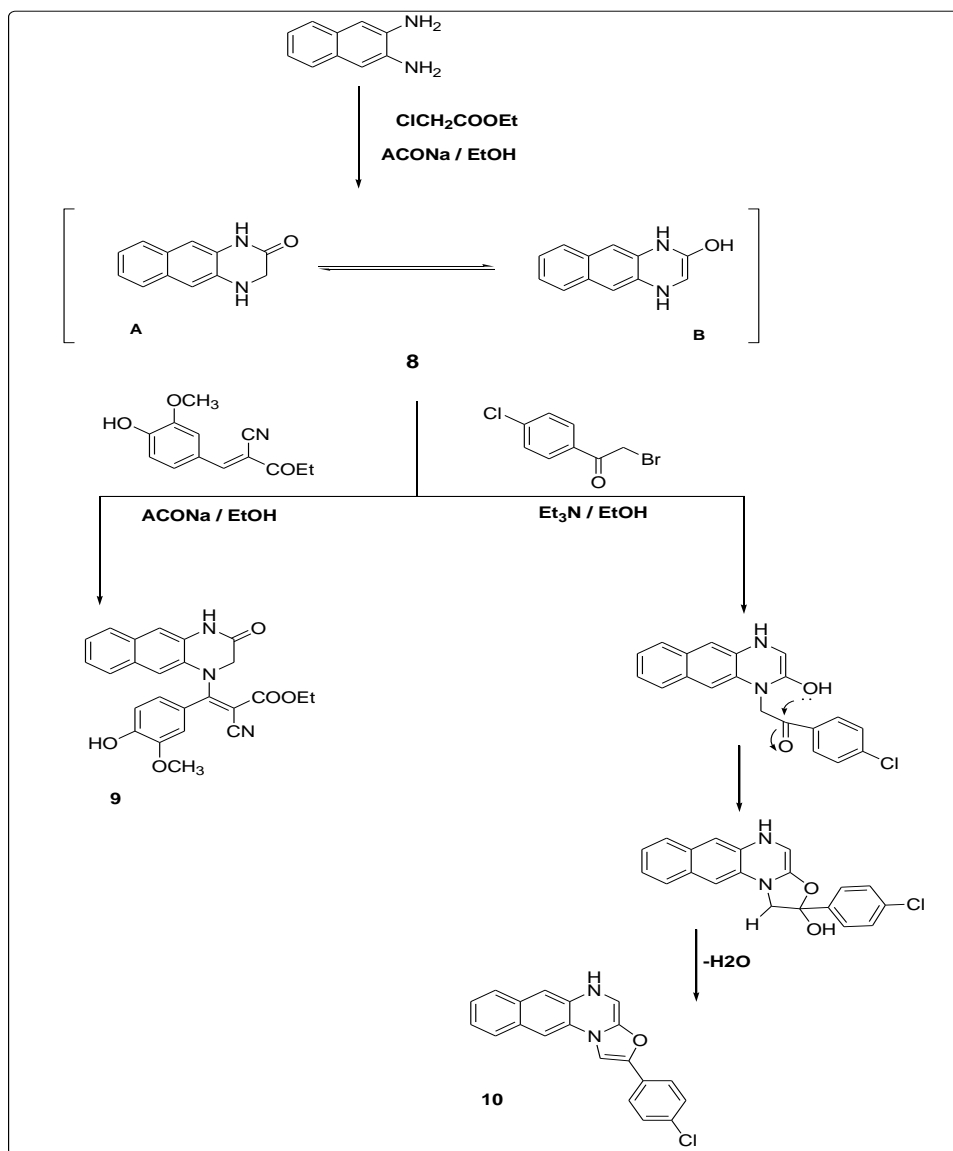
**2.5 Statistical analysis:** Statistical analysis was performed using GraphPad Prism software version 5 (GraphPad software Inc, CA). All data were shown as the average  $\pm$  standard deviation (Mean  $\pm$  SD). Data were analyzed using unpaired t-test and  $P < 0.05$  was considered significant.

### 3. RESULTS AND DISCUSSIONS

**3.1 Chemistry:** The synthetic pathways to obtain the 2-substituted quinoxalines (**3 and 4**) and acetoxy derivatives (**5 and 6**) are outlined in **scheme 1**. 5-bromo-2-hydroxyphenylbromide (**2a**) and 4-aminophenyl bromide (**2b**) were prepared *via* the bromination of 2-hydroxyacetophenone and **1** or 4-aminoacetophenone with bromine in glacial acetic acid through stirring at 60 °C. Cyclocondensation of phenacyl bromide derivatives (**2a, b**) with 1,2-phenylene diamine in acetic acid in the presence of fused sodium acetate under reflux resulted in the formation of 2-(5-bromo-2-hydroxyphenyl)quinoxaline (**3**) and 2-(4-aminophenyl) quinoxaline (**4**). The formation of 2-substituted quinoxalines (**3,4**) were confirmed chemically via the acetylation of compounds **3** and **4** with acetic anhydride under reflux to give 2-(5-bromo-2-acetoxy phenyl) quinoxaline (**5**) and 2-(3,5-dibromo-4-acetyl amino phenyl)quinoxaline (**6**), respectively.



**Scheme 1:** Synthesis of 2-substituted quinoxalines and their acetoxy derivatives (**3-6**).



**Scheme 2:** Synthesis of *N*-substituted 1,2,3,4-tetrahydrobenzo[g]quinoxaline-2-ones (**8** and **9**), 4-hydroxy-1,3-oxazolo[2,1-*b*]benzo[g]quinoxaline (**10**).

The steps involved the synthesis of the second type from 1,2,3,4-tetrahydrobenzo[g]quinoxaline-2-one derivatives (**8-10**) are outlined in **scheme 2**. The starting material naphthalene-2,3-diamine (**7**) was obtained via the reduction of 2,3-dinitronaphthalene with zinc in the presence of hydrochloric acid according to literature procedure [32, 35]. The compound was then reacted with ethyl chloroacetate in ethanol in the presence of fused sodium acetate under reflux to obtain 1,2,3,4-2-oxo-benzo[g]quinoxaline (**8**).

Compound **9** was synthesized via the reaction of compound **8** with ethyl 3-(4-hydroxy-3-methoxyphenyl)-2-cyanoacrylate in the presence of fused sodium acetate in ethanol under reflux. Finally compound **8** was treated with 4-chlorophenyl bromide in ethanol in the presence of triethylamine as a base catalyst to yield 4-*H*-1,3-oxazolo[2,1-*b*]benzo[g]quinoxaline (**10**). The synthesized compounds were confirmed via spectroscopic and elemental analysis.

In <sup>1</sup>HNMR spectrum of compound **8**, the methylene protons (CH<sub>2</sub>) and two NH protons were appeared at (δ 3.77-6.29) and δ 10.59 ppm in the isomer 1,2,3,4-tetrahydrobenzo[g]quinoxaline-2-one (A), while in the

isomer 2-hydroxy-1,4-dihydrobenzo[g] quinoxaline (B), the protons of two NH groups appeared at  $\delta$  4.93 ppm.  $^{13}\text{C}$  NMR spectrum of compound 8 shows the two carbon signals associated to carbonyl attached to methylene group in the isomer A at  $\delta$  167.05 and 46-59 ppm. The aromatic carbon signals in the spectrum for the compound 8 were observed in the expected region.

The structure of compound 9 was confirmed through  $^1\text{H}$  NMR spectrum which showed the absence of NH peak at  $\delta$  6.29 in the spectrum of compound 8. The  $^1\text{H}$  NMR spectrum of compound 9 showed new peaks at  $\delta$  4.29, 3.81 and 1.30 ppm due to the methylene protons as quartet signal,  $\text{OCH}_3$ ,  $\text{NH}_2\text{CO}$  as singlet together and methyl protons as triplet signal. The  $^{13}\text{C}$  NMR spectrum of compound 9 displayed three carbon signals at  $\delta$  163.64, 163.11 and 97.48 due to the two carbonyl ( $\text{C}=\text{O}$ ) and cyano ( $\text{CN}$ ) groups, while the carbon signals of ethoxy ( $\text{CH}_3\text{CH}_2$ ) and methoxy ( $\text{OCH}_3$ ) groups are observed at  $\delta$  62.43, 14.54 ppm and at  $\delta$  53.51 ppm, respectively. In compound 10, the protons of NH group appear at  $\delta$  9.65 ppm as singlet signal in this spectrum. The five protons appear at  $\delta$  7.66-7.71 as multiplet signals refer to the H-aromatic and H-piperazine ring. The protons peak appeared at  $\delta$  8.43-8.46 ppm as doublet signal due to the two protons of aromatic ring, and two singlet signals at  $\delta$  8.27, 8.81 ppm indicated to five protons of aromatic and H-oxazole ring. The  $^{13}\text{C}$  NMR spectrum of compound 10 displayed carbon signal at  $\delta$  150.51 ppm refers to C-O function, the remaining carbon signals of compound 10 are observed in the expected region at  $\delta$  145.33-127.54 ppm.

Mass spectral studies showed a stable molecular ion peak at  $m/z$  302, 377, 342, 419 and  $m/z$  198, corresponding to the molecular formula  $\text{C}_{14}\text{H}_9\text{N}_2\text{BrO}$ ,  $\text{C}_{14}\text{H}_9\text{N}_3\text{Br}_2$ ,  $\text{C}_{16}\text{H}_{11}\text{N}_2\text{BrO}_2$ ,  $\text{C}_{16}\text{H}_{11}\text{N}_3\text{Br}_2\text{O}$  and  $\text{C}_{12}\text{H}_{10}\text{N}_2\text{O}$  for the compounds 3,4,5,6 and 8, respectively. But in the compounds 9 and 10, the mass spectral data for these compounds to showed that found the molecular ion peaks were unstable.

### 3.2 Anti-cancer activity

**3.2.1 *In-vitro* cytotoxicity against MCF-7 cells:** The anticancer activities of the newly synthesized derivatives against MCF-7 cells were investigated using MTT assay where the  $\text{IC}_{50}$  value was calculated for each compound then compared to  $\text{IC}_{50}$  value of Doxorubicin as the reference drug.  $\text{IC}_{50}$  values are shown in Table 1.

**Table 1.  $\text{IC}_{50}$  values ( $\mu\text{g}/\text{mL}$ ) of the tested derivatives (3- 10) against MCF-7 cells.**

Compound code	$\text{IC}_{50}$ ( $\mu\text{g}/\text{mL}$ ) $\pm$ SD
3	21.16 $\pm$ 0.94
4	8.59 $\pm$ 0.38**
5	4.80 $\pm$ 0.21***
6	23.49 $\pm$ 1.04
8	35.78 $\pm$ 1.59
9	3.79 $\pm$ 0.17***
10	6.24 $\pm$ 0.28***
Doxorubicin	11.10 $\pm$ 0.49

$\text{IC}_{50}$  values are means  $\pm$  (SD);  $n=3$ .  $P$  value was calculated using independent t-test for each tested compound vs. Doxorubicin. \*\*\* $P \leq .001$ , \*\* $P \leq .01$ .

Results shown in Table 1 demonstrated that the  $IC_{50}$  of the examined derivatives ranged between  $3.79 \pm 0.17$  and  $35.78 \pm 1.59$   $\mu\text{g/mL}$  suggesting the potential anticancer property of such compounds against MCF-7 cells. Whilst  $IC_{50}$  value recorded for the reference compound Doxorubicin was  $11.10 \pm 0.49$ . Notably,  $IC_{50}$  values recorded for four of the newly synthesized compounds, namely, 9, 5, 10 and 4 were lower than that of the reference compound Doxorubicin highlighting higher cytotoxicity of those compounds towards MCF-7 cells, compared to Doxorubicin. Reported  $IC_{50}$  values for compounds 9, 5, 10 and 4 were  $3.79 \pm 0.17$ ,  $4.80 \pm 0.21$ ,  $6.24 \pm 0.28$  and  $8.59 \pm 0.38$ , respectively. Further statistical analysis comparing the  $IC_{50}$  values of those compounds revealed they were statistically significantly different compared to Doxorubicin ( $P \leq 0.001$  for compounds 9, 5 and 10;  $P \leq 0.01$  for compound 4). Whilst  $IC_{50}$  values recorded for compounds 3, 6, 8 and 11 were higher than that of doxorubicin displaying less potent anticancer activity toward MCF-7 cells.

Moreover, the toxicity of the most promising anticancer derivatives, compounds 5 and 9, were tested on non-carcinogenic epithelial cell line then the selectivity index for each was calculated as shown in Table 2. Results of the current investigation stated that, selectivity index values reported for compounds 5 and 9 were 8.29 and 6.63, respectively. Notably, both investigated compounds demonstrated selectivity index values higher than the recorded value for Doxorubicin that was 1.99. This finding indicated the promising safety profiles for the newly synthesized compounds.

**Table2:  $IC_{50}$  values ( $\mu\text{g/mL}$ ) of the most promising compounds (5 & 9) on MCF-10A non-tumorigenic cells and selectivity indices.**

Compound	MCF-10 <sup>a</sup> ( $\mu\text{g/mL}$ )	Selectivity Index MCF-10 <sup>a</sup> /MCF-7
5	$39.81 \pm 0.31$	8.29
9	$25.16 \pm 0.23$	6.63
Doxorubicin	$22.17 \pm 0.19$	1.99

<sup>a</sup> $IC_{50}$  values are means  $\pm$  (SD) (n = 3).

**3.2.2 Assessment of the inhibition of tubulin polymerization:** Since formation of mitotic spindle is a critical step for cell division, number of drugs such as vinca alkaloids and taxanes targeted this spindle interfering with cell division and inducing cell cycle arrest. Mitotic spindle is an aggregate of microtubules that is composed mainly of tubulin dimers. Notably, certain anticancer drugs function through binding to the tubulin beta protein, an integral component of microtubules, thus causing inhibition of microtubule polymerization with subsequent disturbance of sister chromatids movement/separation.

Further, to elucidate the molecular mechanisms that have underlined the antiproliferative effect of the most promising compound 9, the ability of this compound to inhibit tubulin beta polymerization was assessed and the results were summarized in Table 3. Remarkably, compound 9 demonstrated the highest cytotoxicity on MCF-7 cells in MTT assay alongside low cytotoxicity to non-malignant cells [36].

**Table 3: IC<sub>50</sub> values (ng/mL) for the inhibition of Tubulin beta polymerization following compound 9 treatment.**

Cells	IC <sub>50</sub> (ng/mL)
Compound 9-treated MCF-7 cells	0.814±0.03***
Colchicine-treated MCF-7 cells	1.026±0.022
MCF-7 untreated cells	4.181±0.59

Values are means ± (SD) (n = 3). *P* value was calculated using independent t-test for compound 9 and Doxorubicin vs. control non-treated MCF-7 cells. \*\*\**P* ≤ 0.001.

Results shown in table 3 indicated that the novel compound 9 exerted statistically significant inhibitory effect of tubulin beta polymerization with IC<sub>50</sub> of 0.814±0.03 (ng/mL), *P* ≤ 0.001, compared to Colchicine-treated MCF-7 cells. Whilst the reference compound Colchicine induced inhibition of tubulin beta polymerization with IC<sub>50</sub> (ng/mL) of 1.026±0.022.

The results of the current study displayed the ability of the tested compound 9 to exert its anticancer activity against MCF-7 cells through the inhibition of tubulin beta polymerization, therefore, molecular modelling study was conducted to confirm this finding. The compound 9 containing amide function (CONH), phenolic-OH, methoxy (OCH<sub>3</sub>), cyano and carbonyl of ester groups, which interact with amino acids via the hydrogen bond and hydrophobic binding.

**3.3 Molecular docking studies:** After molecular docking study, compound 9 and colchicine share the same binding site in the tubulin Fig. 7. Colchicine showed two hydrogen bonds with Val 181, Cys241 as well as many hydrophobic interactions (Table 4). The hydrophobic interactions include p-sulfur with Met259, p-sigma with Leu255 and Van der Waals interactions (Fig. 8). Similarly, compound 9 binding varies between hydrophobic interactions and hydrogen bonding (Fig. 9) which is reflected by the docking scores, see Table 4. The studied compound 9 forms four hydrogen bonds with amino acid residues Asn101, Ser178, Leu248 and Asn249 of the active site of tubulin. Compound 9 also showed many Van der Waals interactions and two p-sigma with Leu248 and Leu255.

**Table 4: The binding modes and docking scores for Colchicine and Compound 9 into tubulin active site.**

Compound	H-bonds	Hydrophobic interaction	Docking score(Å)
Colchicine	Val 181, Cys241	Cys241, Leu242, Leu248, Ala250, Leu255, Met259, Ala316, Val318, Lys352, Ala354, Ile378	-8.7
9	Asn101, Ser178, Leu248, Asn249	Cys241, Leu248, Lys254, Leu255, Ala316, Ala354, Ile378	-9.5

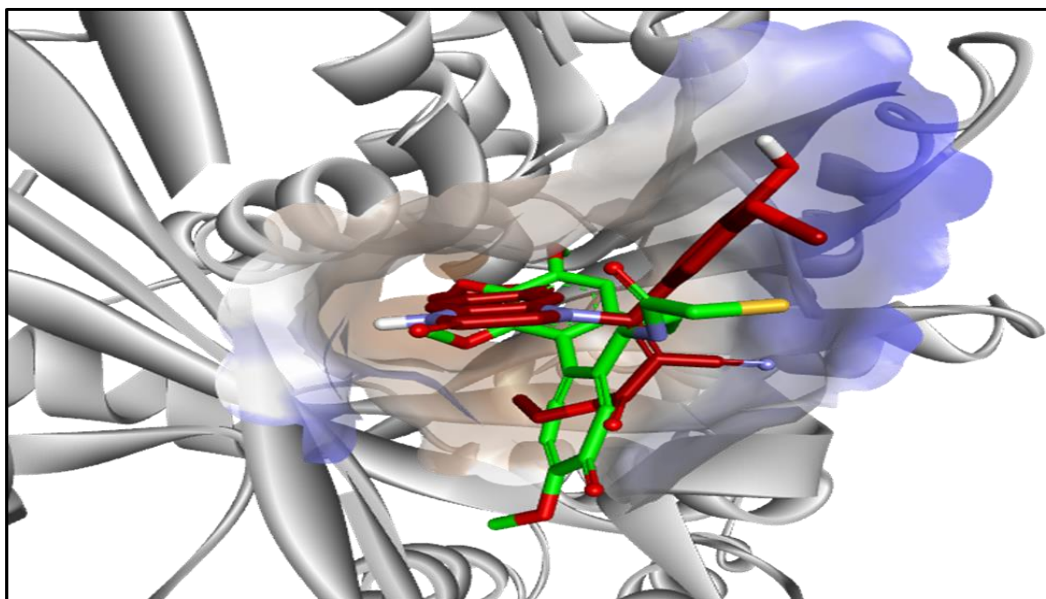


**Fig. 7: Overly of Colchicine and Compound 9 into the active site of tubulin receptor.**

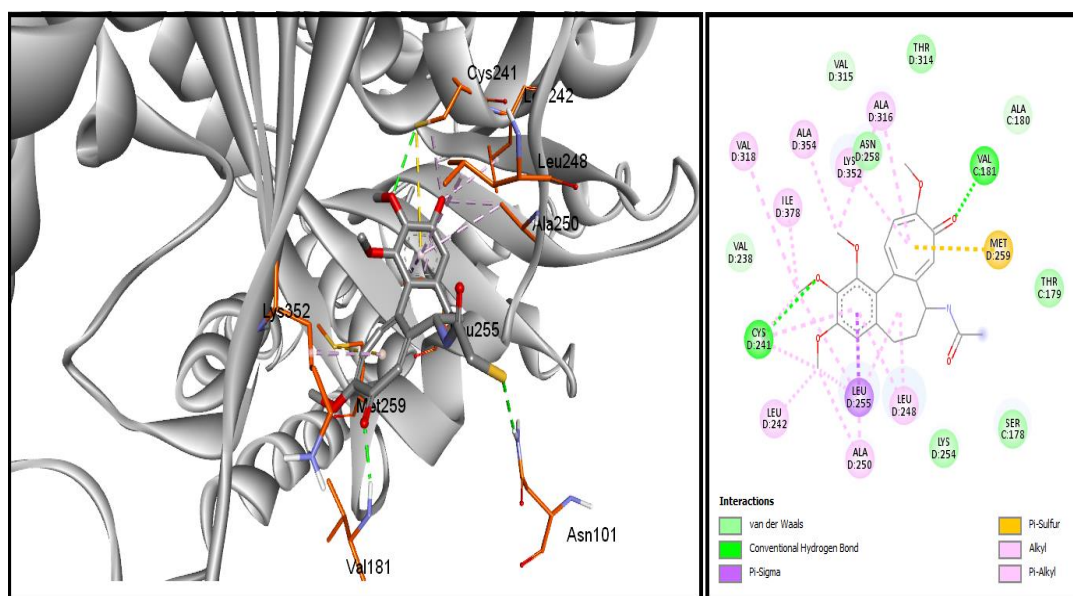


**Fig. 8: Interaction visualization: 3D active site view (left) and 2D schematic view (right), of Colchicine into the active site of tubulin receptor.**

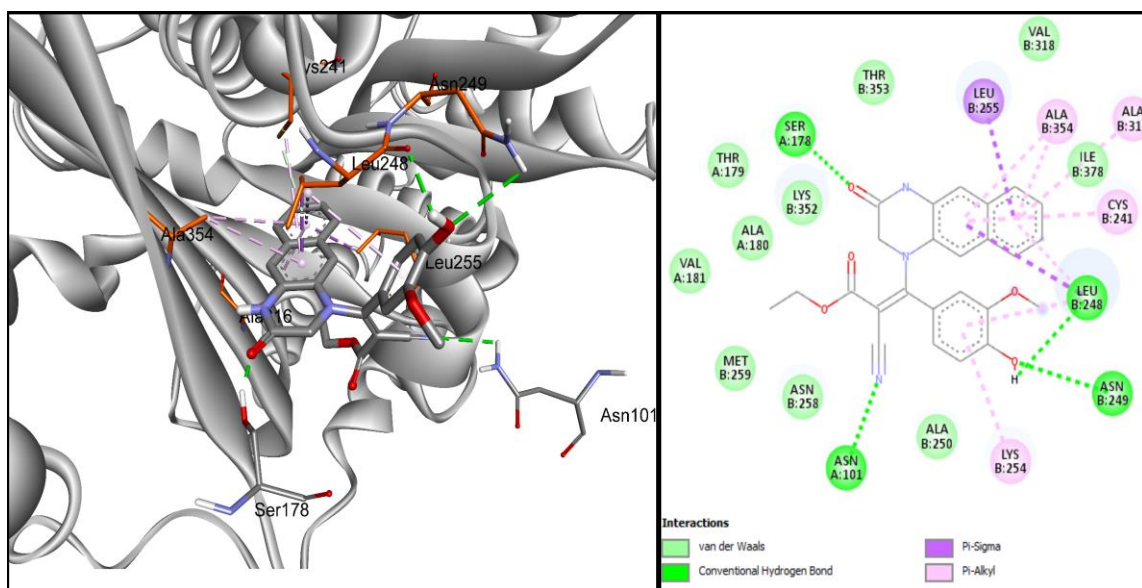


**Fig. 9: Interaction visualization: 3D active site view (left) and 2D schematic view (right), of Compound 9 into the active site of tubulin receptor.**

#### 4. CONCLUSION

In one such attempt adopting molecular hybridization strategy, we synthesized as many as seven derivatives of the quinoxaline derivatives compounds (3-6) bearing substituted aromatic ring and fused quinoxaline derivatives compounds (8-10). They were then tested for potential cytotoxicity by using MCF-7 cell line, a widely accepted in-vitro model for carcinoma. The results of this study revealed that one in every of those derivatives, compound 9, at an occasional concentration of  $3.79 \pm 0.17 \mu\text{g/mL}$ , successfully induced significant cytotoxicity against MCF-7 cells. This work administered further investigations to elucidate the protection moreover as molecular mechanisms underlying this observation.

Firstly, the cytotoxicity of the foremost promising compound 9 toward MCF-10a non-carcinogenic cell line where the tested compound displayed good safety profile toward the standard cells as evidenced by the recorded SI of 6.63, whilst the reference drug Doxorubicin showed SI of 1.99. Secondly, the pliability of the tested compound 9 to inhibit tubulin beta polymerization was assessed demonstrating significant suppression in tubulin beta polymerization in compound 9 -treated cells. Furthermore, docking of compound 9 was performed on tubulin binding sites confirming its binding interactions to resemble that of the reference ligands. Our findings suggest that the hybridized compound 9 may be a promising anticancer drug against carcinoma cells that represent promising lead for future investigations.

#### 5. REFERENCES

- [1] R. L. Siegel, K. D. Miller, N. S. Wagle, and A. Jemal, "Cancer statistics, 2023," *CA Cancer J Clin*, vol. 73, no. 1, pp. 17–48, Jan. 2023, doi: 10.3322/CAAC.21763.
- [2] N. Eliyatkin, E. Yalcin, B. Zengel, S. Aktaş, and E. Vardar, "Molecular Classification of Breast Carcinoma: From Traditional, Old-Fashioned Way to A New Age, and A New Way," *Journal of Breast Health*, vol. 11, no. 2, pp. 59–66, 2015, doi: 10.5152/tjbh.2015.1669.

- [3] A. Szymiczek, A. Lone, and M. R. Akbari, "Molecular intrinsic versus clinical subtyping in breast cancer: A comprehensive review," *Clinical Genetics*, vol. 99, no. 5. 2021. doi: 10.1111/cge.13900.
- [4] T. Mitchison and M. Kirschner, "Dynamic instability of microtubule growth," *Nature*, vol. 312, no. 5991, 1984, doi: 10.1038/312237a0.
- [5] G. Breuzard *et al.*, "Molecular mechanisms of Tau binding to microtubules and its role in microtubule dynamics in live cells," *J Cell Sci*, vol. 126, no. 13, 2013, doi: 10.1242/jcs.120832.
- [6] M. A. Jordan and L. Wilson, "Microtubules as a target for anticancer drugs," *Nature Reviews Cancer*, vol. 4, no. 4. 2004. doi: 10.1038/nrc1317.
- [7] B. D. Lindner *et al.*, "N-Fused quinoxalines and benzoquinoxalines as attractive emitters for organic light emitting diodes," *J Mater Chem C Mater*, vol. 1, no. 36, pp. 5718–5724, 2013, doi: 10.1039/C3TC30828F.
- [8] R. Iemura, T. Kawashima, T. Fukuda, K. Ito, and G. Tsukamoto, "Synthesis of 2-(4-substituted-1-piperazinyl)benzimidazoles as H1-antihistaminic agents," *J Med Chem*, vol. 29, no. 7, pp. 1178–1183, Jul. 1986, doi: 10.1021/jm00157a010.
- [9] E. B. Faulkner and R. J. Schwartz, *High performance pigments*. John Wiley & Sons, 2009.
- [10] R. Sarges, H. R. Howard, R. G. Browne, L. A. Lebel, P. A. Seymour, and B. K. Koe, "4-Amino[1,2,4]triazolo[4,3-a]quinoxalines. A novel class of potent adenosine receptor antagonists and potential rapid-onset antidepressants," *J Med Chem*, vol. 33, no. 8, pp. 2240–2254, Aug. 1990, doi: 10.1021/jm00170a031.
- [11] O. O. Ajani, "Present status of quinoxaline motifs: Excellent pathfinders in therapeutic medicine," *Eur J Med Chem*, vol. 85, pp. 688–715, Oct. 2014, doi: 10.1016/j.ejmech.2014.08.034.
- [12] S. D. Undevia *et al.*, "A phase I and pharmacokinetic study of the quinoxaline antitumour Agent R(+)-XK469 in patients with advanced solid tumours," *Eur J Cancer*, vol. 44, no. 12, pp. 1684–1692, Aug. 2008, doi: 10.1016/j.ejca.2008.05.018.
- [13] V. G. Ugale and S. B. Bari, "Quinazolines: New horizons in anticonvulsant therapy," *Eur J Med Chem*, vol. 80, pp. 447–501, Jun. 2014, doi: 10.1016/j.ejmech.2014.04.072.
- [14] G. Grover and S. G. Kini, "Synthesis and evaluation of new quinazolone derivatives of nalidixic acid as potential antibacterial and antifungal agents," *Eur J Med Chem*, vol. 41, no. 2, pp. 256–262, Feb. 2006, doi: 10.1016/j.ejmech.2005.09.002.
- [15] A. K. Tiwari, V. K. Singh, A. Bajpai, G. Shukla, S. Singh, and A. K. Mishra, "Synthesis and biological properties of 4-(3H)-quinazolone derivatives," *Eur J Med Chem*, vol. 42, no. 9, pp. 1234–1238, Sep. 2007, doi: 10.1016/j.ejmech.2007.01.002.
- [16] S. Bhattacharya and P. Chaudhuri, "Medical Implications of Benzimidazole Derivatives as Drugs Designed for Targeting DNA and DNA Associated Processes," *Curr Med Chem*, vol. 15, no. 18, pp. 1762–1777, Aug. 2008, doi: 10.2174/092986708785133013.

- [17] R. Robinson and R. Taylor, "Quinoxaline Synthesis from  $\alpha$ -Hydroxy Ketones via a Tandem Oxidation Process Using Catalysed Aerobic Oxidation," *Synlett*, vol. 2005, no. 06, pp. 1003–1005, Mar. 2005, doi: 10.1055/s-2005-864830.
- [18] M. M. Ibrahim, D. Grau, F. Hampel, and S. B. Tsogoeva, " $\alpha$ -Nitro Epoxides in Organic Synthesis: Development of a One-Pot Organocatalytic Strategy for the Synthesis of Quinoxalines," *European J Org Chem*, vol. 2014, no. 7, pp. 1401–1405, Mar. 2014, doi: 10.1002/ejoc.201301591.
- [19] K. Kumar, S. R. Mudshinge, S. Goyal, M. Gangar, and V. A. Nair, "A catalyst free, one pot approach for the synthesis of quinoxaline derivatives via oxidative cyclisation of 1,2-diamines and phenacyl bromides," *Tetrahedron Lett*, vol. 56, no. 10, pp. 1266–1271, Mar. 2015, doi: 10.1016/j.tetlet.2015.01.138.
- [20] R. H. Crabtree, "Homogeneous Transition Metal Catalysis of Acceptorless Dehydrogenative Alcohol Oxidation: Applications in Hydrogen Storage and to Heterocycle Synthesis," *Chem Rev*, vol. 117, no. 13, pp. 9228–9246, Jul. 2017, doi: 10.1021/acs.chemrev.6b00556.
- [21] A. Corma, J. Navas, and M. J. Sabater, "Advances in One-Pot Synthesis through Borrowing Hydrogen Catalysis," *Chem Rev*, vol. 118, no. 4, pp. 1410–1459, Feb. 2018, doi: 10.1021/acs.chemrev.7b00340.
- [22] S. Shee, K. Ganguli, K. Jana, and S. Kundu, "Cobalt complex catalyzed atom-economical synthesis of quinoxaline, quinoline and 2-alkylaminoquinoline derivatives," *Chemical Communications*, vol. 54, no. 50, pp. 6883–6886, 2018, doi: 10.1039/C8CC02366B.
- [23] R. Zhang, Y. Qin, L. Zhang, and S. Luo, "Oxidative Synthesis of Benzimidazoles, Quinoxalines, and Benzoxazoles from Primary Amines by ortho-Quinone Catalysis," *Org Lett*, vol. 19, no. 20, pp. 5629–5632, Oct. 2017, doi: 10.1021/acs.orglett.7b02786.
- [24] T. Hille, T. Irrgang, and R. Kempe, "The Synthesis of Benzimidazoles and Quinoxalines from Aromatic Diamines and Alcohols by Iridium-Catalyzed Acceptorless Dehydrogenative Alkylation," *Chemistry - A European Journal*, vol. 20, no. 19, pp. 5569–5572, May 2014, doi: 10.1002/chem.201400400.
- [25] C. S. Cho and S. G. Oh, "A new ruthenium-catalyzed approach for quinoxalines from o-phenylenediamines and vicinal-diols," *Tetrahedron Lett*, vol. 47, no. 32, pp. 5633–5636, Aug. 2006, doi: 10.1016/j.tetlet.2006.06.038.
- [26] K. Das, A. Mondal, and D. Srimani, "Phosphine free Mn-complex catalysed dehydrogenative C–C and C–heteroatom bond formation: a sustainable approach to synthesize quinoxaline, pyrazine, benzothiazole and quinoline derivatives," *Chemical Communications*, vol. 54, no. 75, pp. 10582–10585, 2018, doi: 10.1039/C8CC05877F.
- [27] P. Daw, A. Kumar, N. A. Espinosa-Jalapa, Y. Diskin-Posner, Y. Ben-David, and D. Milstein, "Synthesis of Pyrazines and Quinoxalines via Acceptorless Dehydrogenative Coupling Routes Catalyzed by Manganese Pincer Complexes," *ACS Catal*, vol. 8, no. 9, pp. 7734–7741, Sep. 2018, doi: 10.1021/acscatal.8b02208.

- [28] T. Kaushal, G. Srivastava, A. Sharma, and A. Singh Negi, "An insight into medicinal chemistry of anticancer quinoxalines," *Bioorg Med Chem*, vol. 27, no. 1, pp. 16–35, Jan. 2019, doi: 10.1016/j.bmc.2018.11.021.
- [29] J. Qi *et al.*, "Synthesis and biological evaluation of N-substituted 3-oxo-1,2,3,4-tetrahydroquinoxaline-6-carboxylic acid derivatives as tubulin polymerization inhibitors," *Eur J Med Chem*, vol. 143, pp. 8–20, Jan. 2018, doi: 10.1016/j.ejmech.2017.08.018.
- [30] A. H. Abu Almaaty *et al.*, "5-Aryl-1-Arylideneamino-1H-Imidazole-2(3H)-Thiones: Synthesis and In Vitro Anticancer Evaluation," *Molecules*, vol. 26, no. 6, p. 1706, Mar. 2021, doi: 10.3390/molecules26061706.
- [31] A. A. E. Mourad, Y. W. Rizzk, I. Zaki, F. Z. Mohammed, and M. El Behery, "Synthesis and cytotoxicity screening of some synthesized hybrid nitrogen molecules as anticancer agents," *J Mol Struct*, vol. 1242, p. 130722, Oct. 2021, doi: 10.1016/j.molstruc.2021.130722.
- [32] I. Zaki, S. A. Abu El-ata, E. Fayad, O. A. Abu Ali, A. H. Abu Almaaty, and A. S. Saad, "Evaluation of Synthetic 2,4-Disubstituted-benzo[g]quinoxaline Derivatives as Potential Anticancer Agents," *Pharmaceuticals*, vol. 14, no. 9, p. 853, Aug. 2021, doi: 10.3390/ph14090853.
- [33] S. Jarre *et al.*, "Synthesis, characterization, potential anticancer activity, and molecular docking studies of Fe(II)Prolinedithiocarbamate complex on MCF-7 breast cancer cell lines," *Egypt. J. Chem*, vol. 66, no. 6, pp. 61–67, 2023, doi: 10.21608/EJCHEM.2022.149508.6466
- [34] "Human Beta-tubulin ELISA Kit (ab245722) | Abcam." Accessed: Feb. 19, 2024. [Online]. Available: <https://www.abcam.com/products/elisa/human-beta-tubulin-elisa-kit-ab245722.html>
- [35] R. B. G. Ravelli *et al.*, "Insight into tubulin regulation from a complex with colchicine and a stathmin-like domain," *Nature*, vol. 428, no. 6979, 2004, doi: 10.1038/nature02393.
- [36] O. Trott and A. J. Olson, "AutoDock Vina: Improving the speed and accuracy of docking with a new scoring function, efficient optimization, and multithreading," *J Comput Chem*, 2009, doi: 10.1002/jcc.21334.
- [37] N. M. Seleem, H. K. Abd El Latif, M. A. Shaldam, and A. El-Ganiny, "Drugs with new lease of life as quorum sensing inhibitors: for combating MDR *Acinetobacter baumannii* infections," *European Journal of Clinical Microbiology and Infectious Diseases*, vol. 39, no. 9, 2020, doi: 10.1007/s10096-020-03882-z.